0026-895X/04/6606-1478–1490$20.00
MOLECULAR PHARMACOLOGY
Copyright © 2004 The American Society for Pharmacology and Experimental Therapeutics
Mol Pharmacol 66:1478–1490, 2004

Vol. 66, No. 6
3400/1186548
Printed in U.S.A.

Evidence That Mitogen-Activated Protein Kinase Phosphatase-1 Induction by Proteasome Inhibitors Plays an Antiapoptotic Role

George W. Small, Yue Y. Shi, Natalie A. Edmund, Sivagurunathan Somasundaram,[1] Dominic T. Moore, and Robert Z. Orlowski

The Lineberger Comprehensive Cancer Center (G.W.S., Y.Y.S., N.A.E., S.S., D.T.M., R.Z.O.) and the Department of Medicine, Division of Hematology/Oncology (R.Z.O.), University of North Carolina at Chapel Hill, Chapel Hill, North Carolina

Received June 1, 2004; accepted September 23, 2004

ABSTRACT

Inhibitors of the proteasome, a multicatalytic proteinase complex responsible for intracellular proteolysis, activate programmed cell death in part through the c-Jun-N-terminal kinase (JNK). Proteasome inhibitors also induce mitogen-activated protein kinase phosphatase-1 (MKP-1), however, which can inactivate JNK, and we therefore considered the hypothesis that MKP-1 induction may be antiapoptotic. Overexpression of MKP-1 in A1N4-*myc* human mammary epithelial and BT-474 breast carcinoma cells decreased proteasome inhibitor-mediated apoptosis. On the other hand, BT-474 cells stably expressing an MKP-1 small interfering RNA (siMKP-1) and MKP-1 knockout mouse embryo fibroblasts underwent enhanced apoptosis compared with their respective controls. MKP-1-mediated inhibition of apoptosis was associated with decreased phospho-JNK levels, whereas MKP-1 suppression or inactivation enhanced phospho-JNK. Anthracyclines repress MKP-1 transcription, suggesting that they could enhance proteasome inhibitor-mediated apoptosis. Such combinations induced increased cell death in association with enhanced phospho-JNK and decreased MKP-1 levels. Inhibition of JNK signaling decreased the proapoptotic activity of the anthracycline/proteasome inhibitor regimen. Xenograft studies showed the combination was more effective at inducing tumor growth delay, associated with suppression of MKP-1 and enhancement of apoptosis and phospho-JNK. Infection of anthracycline/proteasome inhibitor-treated A1N4-*myc* cells with Adenoviral-MKP-1 suppressed apoptosis and phospho-JNK. Finally, the anthracycline/proteasome inhibitor regimen activated apoptosis and phospho-JNK to a greater extent in BT-474/siMKP-1 cells than controls. These findings for the first time demonstrate that proteasome inhibitor-mediated induction of MKP-1 is antiapoptotic through inhibition of JNK. Furthermore, they suggest that a proteasome inhibitor/anthracycline regimen holds potential for enhanced antitumor activity in part through repression of MKP-1, supporting clinical evaluation of such combinations.

The majority of regulated intracellular eukaryotic protein turnover occurs through the ubiquitin-proteasome pathway (Ciechanover et al., 2000). Coordinated function of this pathway results first in the labeling of target proteins by the ubiquitin conjugation system to form polyubiquitin chains. Once so tagged, these proteins become substrates for proteolysis by the multicatalytic proteinase complex, or proteasome, a macromolecular structure with up to five different proteolytic activities (Orlowski and Wilk, 2000). These proteases generate oligopeptides from target proteins, which exit the proteasome and are then further degraded into their constituent amino acids by endopeptidases and aminopeptidases. Recent studies have validated the proteasome as a target for cancer therapy, because small molecule inhibitors of this complex have antitumor activity, in part through the activation of programmed cell death (Voorhees et al., 2003).

Support for these studies (to R.Z.O.) came from Department of Defense Breast Cancer Research Program Grant BC991049, Leukemia and Lymphoma Society Grant R6206-02, National Cancer Institute Grant R01-CA102278, the Ellence Research Fund, and the Lineberger Comprehensive Cancer Center SPORE for Breast Cancer Grant P50-CA-58223. Support for the phase I trial of bortezomib and pegylated liposomal doxorubicin was provided by Millennium Pharmaceuticals, Inc. (Cambridge, MA) and from the General Clinical Research Centers Program of the Division of Research Resources, National Institutes of Health (RR00046).

[1] Current address: University of Houston-Victoria, School of Arts and Science, Victoria, Texas 77901-5731.

Article, publication date, and citation information can be found at http://molpharm.aspetjournals.org.
doi:10.1124/mol.104.003400.

ABBREVIATIONS: NF, nuclear factor; JNK, c-Jun-N-terminal kinase; MAPK, mitogen-activated protein kinase; MKP, mitogen-activated protein kinase phosphatase; ERK, extracellular signal-regulated kinase; siRNA, small interfering RNA; PS-341, bortezomib; Z-LLF-CHO, *N*-benzyloxycarbonyl-leucyl-leucyl-phenylalanyl-aldehyde; PMSF, phenylmethylsulfonyl fluoride; PBS, phosphate-buffered saline; MEF, mouse embryo fibroblast; DP, dominant-positive; ERK, extracellular signal-regulated kinase; CMV, cytomegalovirus; ss, scrambled sequence; GFP, green fluorescent protein; DN, dominant-negative; ELISA, enzyme-linked immunosorbent assay; FACS, fluorescence-activated cell sorting; HSC, heat shock cognate protein; siMKP-1, small interfering RNA targeting MKP-1; ssMKP-1, small interfering RNA with a scrambled sequence that does not target MKP-1; HSP, heat shock protein.

One such inhibitor, bortezomib, previously known as PS-341 (Adams et al., 1999), has entered clinical trials and encouraging results have been obtained in both phase I (Orlowski et al., 2002b) and phase II studies (Richardson et al., 2003) in patients with multiple myeloma. Additional trials are ongoing to define its full utility in other tumor types, including breast cancer, where there is a strong preclinical rationale for targeting the proteasome (Orlowski and Dees, 2003).

Proteasome inhibitors probably affect many cell death-associated signal transduction pathways. One of the more important of these is nuclear factor κ-B (NF-κB), whose nuclear translocation is inhibited, thereby decreasing NF-κB-dependent transcription of antiapoptotic Bcl-2 homologs such as Bcl-x_L (Voorhees et al., 2003). Another important pathway involved in proteasome inhibitor-mediated apoptosis is the c-Jun-N-terminal kinase (JNK). Inhibition of the proteasome resulted in the sustained activation of JNK in several model systems, whereas blockade of JNK/c-Jun/activator protein-1 function decreased apoptosis (Meriin et al., 1998; Hideshima et al., 2003; Yang et al., 2004). JNK activation by a variety of stimuli induces mitochondrial release of cytochrome *c* (Tournier et al., 2000), at least in part by promoting Bax translocation to mitochondria through phosphorylation of 14-3-3 proteins (Tsuruta et al., 2004). This mechanism seems also to be used by proteasome inhibitors in their induction of apoptosis (Pei et al., 2003; Yu et al., 2004).

Another consequence of proteasome inhibition is the transcriptional induction of mitogen-activated protein kinase (MAPK) phosphatase (MKP)-1 (Orlowski et al., 2002a). MKP-1 was originally identified based on its specificity toward the p44/42 MAPK pathway, also called the extracellular-signal-regulated kinases (ERK), but MKP-1 is a general MAPK phosphatase that can also dephosphorylate JNK (Kelly and Chu, 2000). Indeed, in some model systems, MKP-1 demonstrates a substrate preference for JNK over other targets (Liu et al., 1995; Franklin and Kraft, 1997). The ability of MKP-1 to inactivate JNK has been linked in some systems to inhibition of apoptosis caused by stimuli such as ultraviolet light (Liu et al., 1995; Franklin et al., 1998; Guo et al., 1998), and MKP-1 may be a mediator of glucocorticoid-induced survival signals in breast epithelial cells (Wu et al., 2004). This led us to consider the possibility that proteasome inhibitors are limited in their ability to induce programmed cell death by their own induction of MKP-1, and that inhibition of MKP-1 may enhance the efficacy of this novel class of agents.

In the current report, we present evidence that either transient or stable over-expression of MKP-1 inhibited the ability of proteasome inhibitors to induce apoptosis in human mammary epithelial and breast carcinoma cells. Inhibition of MKP-1 by stable expression of a small interfering (si) RNA, or targeted disruption of MKP-1, resulted in cell lines that were more sensitive to proteasome inhibitor-mediated apoptosis. Overexpression of MKP-1 decreased activation of JNK, whereas inhibition of MKP-1 enhanced phospho-JNK levels. Anthracyclines have recently been shown to inhibit MKP-1 (Small et al., 2003), and combinations of a proteasome inhibitor and an anthracycline were therefore tested. These combinations resulted in enhanced apoptosis, repression of MKP-1, and increased activation of JNK in both in vitro and in vivo model systems and enhanced in vivo antitumor efficacy. JNK activation by this novel, rational combination was important because inhibition of signaling through this pathway decreased apoptosis. Finally, inhibition of MKP-1 was found to enhance apoptosis and JNK activation because of the proteasome inhibitor/anthracycline regimen, whereas forced overexpression of MKP-1 suppressed both apoptosis and phospho-JNK levels. Taken together, these studies for the first time show that the induction of MKP-1 by proteasome inhibition is antiapoptotic through down-regulation of JNK activity and suggest that regimens containing a proteasome inhibitor and an anthracycline merit further study in vivo.

Materials and Methods

Materials. The proteasome inhibitor PS-341 (bortezomib; Velcade) was provided by Millennium Pharmaceuticals, Inc. (Cambridge, MA); *N*-benzyloxycarbonyl-leucyl-leucyl-phenylalanyl-aldehyde (Z-LLF-CHO) was prepared as described previously (Orlowski et al., 2002a). Doxorubicin was from Sigma-Aldrich Co. (St. Louis, MO); epirubicin (Ellence; Pharmacia and Upjohn, Peapack, NJ) was from the University of North Carolina at Chapel Hill Memorial Hospital pharmacy, and pegylated liposomal doxorubicin (Doxil) was from Ortho Biotech Products, L.P. (Bridgewater, NJ). Phosphatase inhibitors deltamethrin and nodularin were from Calbiochem-Novabiochem Corp. (San Diego, CA); sodium orthovanadate was from Sigma-Aldrich. Complete protease cocktail was from Roche Applied Science (Indianapolis, IN); phenylmethylsulfonyl fluoride (PMSF) was from Fisher Scientific Co. (Fair Lawn, NJ). Stock solutions were prepared in 100% isopropanol (Mallinckrodt Baker, Inc., Paris, KY) for PMSF, Dulbecco's phosphate-buffered saline (PBS) (from the Lineberger Comprehensive Cancer Center (LCCC) Tissue Culture Facility) for sodium orthovanadate, or dimethyl sulfoxide for all others, and stored at −20°C. These reagents were used at concentrations indicated in the text, with a final vehicle concentration that did not exceed 0.5% (v/v). Restriction enzymes HindIII and EcoRV, as well as T4 DNA ligase and the appropriate enzyme buffers, were from New England Biolabs, Inc. (Beverly, MA). Blasticidin S, hygromycin, and puromycin were from Calbiochem-Novabiochem Corp., Geneticin/G418 sulfate was from Invitrogen (Carlsbad, CA); doxycycline was from Sigma-Aldrich Co. All other chemicals, unless otherwise indicated, were obtained from Fisher Scientific.

Cell Lines and Cell Culture. A1N4-*myc* human mammary epithelial cells transformed by the *c-myc* oncogene, BT-474 breast carcinoma cells, and mouse embryo fibroblasts (MEFs) from homozygous MKP-1 knockout mice, as well as wild-type control mice, were propagated as described previously (Small et al., 2003). Construction of the A1N4-*myc*- (Orlowski et al., 2002a) and BT-474-based cell lines (Small et al., 2003) expressing dominant-positive (DP) ERK-2 was described previously. The analogous DP-ERK-1 mutant tagged with hemagglutinin was kindly provided by Dr. Channing Der (University of North Carolina at Chapel Hill, Chapel Hill, NC), cloned into pLNCX (BD Biosciences Clontech, Palo Alto, CA), where expression is driven by the human cytomegalovirus (CMV) immediate early promoter, and verified by sequencing (DNA Sequencing Core Facility, LCCC). BT-474/DP-ERK-1/2 was prepared by transfecting BT-474/DP-ERK-2 with pLNCX-DP-ERK-1 as described previously (Small et al., 2003), followed by selection in media containing Geneticin/G418 sulfate. Colonies were screened for expression of both mutant ERKs by Western blotting as described below, using a murine anti-HA monoclonal antibody (Santa Cruz Biotechnology, Inc., Santa Cruz, CA).

To prepare cell lines stably over-expressing MKP-1, BT-474 cells were transfected with pcDNA3 (Invitrogen) as a control or with pcDNA3/MKP-1, both kindly provided by Dr. Philip J. S. Stork (Oregon Health Sciences University, Portland, OR). After transfection using the Gene-PORTER reagent (Gene Therapy Systems, San Diego, CA) according to the manufacturer's specifications, stable

clones were selected by culturing in media containing Geneticin/G418 sulfate, and screened by Western blotting. A1N4-*myc* cells can be transfected only with viral-mediated delivery systems and were therefore induced to overexpress MKP-1 by transient transfection using an Adenoviral system as described below. The construction of BT-474 cell lines stably expressing either an siRNA molecule targeting MKP-1 (BT-474/siMKP-1) or a control scrambled sequence (ss) RNA (BT-474/ssMKP-1) was described previously (Small et al., 2003).

Retroviral vectors directing the doxycycline-inducible expression from pLRT of either green fluorescent protein (GFP) as a control, or the dominant-negative (DN) c-Jun mutant TAM-67, were kindly provided as viral supernatants by Dr. Michael Birrer (National Cancer Institute). A1N4-*myc* cells were infected under standard conditions, selected for blasticidin S resistance, and screened by inducing with doxycycline at 10 μg/ml, followed by Western blotting of cell extracts for the protein of interest. BT-474 cells constitutively expressing DN-c-Jun were prepared by transfecting with pcDNA3.1-TAM-67 (also kindly provided by Dr. Michael Birrer). DN-JNK-1α tagged with hemagglutinin from pLNCX (kindly provided by Dr. Tomas Berl; University of Colorado Health Sciences Center) was recloned into pcDNA3.1, and BT-474 cells were then transfected, selected, and screened as described above.

Adenoviral MKP-1 Preparation and Use. A recombinant adenovirus plasmid designed to induce expression of both MKP-1 and GFP was constructed using the AdEasy vector system (Stratagene, La Jolla, CA). In brief, the 2-kilobase pair HindIII-EcoRV fragment from pcDNA3/MKP-1 containing the human MKP-1 gene was ligated into the shuttle vector pAdTrack-CMV, which uses the CMV promoter for protein expression in mammalian cells. Recombinant adenovirus (Ad-GFP/MKP-1) was produced by homologous recombination of the shuttle vector with the replication-deficient pAdEasy vector, and adenoviral stocks were generated in human embryonic kidney 293 cells by the LCCC Gene Therapy Core Facility. As a control, adenovirus inducing only GFP (Ad-GFP) expression was used and differed from Ad-GFP/MKP-1 only in the lack of the MKP-1 gene insert.

For adenoviral infection, cell lines were plated in Costar 3595 96-well plates (Corning Inc., Corning, NY) at a density of 0.5×10^3 cells per well or in Falcon 3047 24-well plates (BD Biosciences Discovery Labware, Bedford, MA) at a density of 1.0×10^5 cells per well. Cells were then allowed to recover overnight and exposed to viral particles using a multiplicity of infection that was controlled to yield 80 to 100% infection, based on GFP expression evaluated by immunofluorescence microscopy using an ultraviolet Zeiss Axioplan fluorescence microscope (Carl Zeiss Optical, Inc., Chester, VA). Treatments of interest were then added 24 h later in an equal volume of fresh media, and cells were harvested for analysis by Western blotting or apoptosis assays after an additional 18 h as described below.

Apoptosis Assays. Induction of programmed cell death was evaluated primarily using the apoptosis-specific Cell Death Detection ELISA^{PLUS} kit (Roche Applied Science, Indianapolis, IN). This assay detects apoptotic DNA damage using a biotinylated anti-histone antibody that tethers oligonucleosome fragments to a streptavidin-coated well, followed by a peroxidase-conjugated anti-DNA antibody, and was performed according to the manufacturer's specifications. Spectrophotometric data at a wavelength of 405 nm, with a reference of 490 nm, were acquired on a MAXline Vmax kinetic microplate reader (Molecular Devices, Sunnyvale, CA). The enhancement of apoptosis induced by each condition was calculated in relation to parallel control cells, which received solvent alone, and tabulated in KaleidaGraph (ver. 3.0.1; Synergy Software, Reading, PA). Mean percentages and S.E.M. were then calculated and plotted in KaleidaGraph. Experimental conditions were chosen in part based on prior studies of the effects of proteasome inhibitors (Orlowski et al., 2002a) and anthracyclines (Small et al., 2003) on the respective cell lines, and also to allow for the analysis of apoptosis data in the linear range of the assay being used. In experiments with proteasome inhibitors alone, and in combination with anthracyclines, an 18-hour incubation was generally used, unless indicated otherwise.

As a confirmatory assay in certain experiments, apoptosis was also evaluated by determining the proportion of cells with a sub-G_1 DNA content. After the treatments of interest, approximately 2×10^6 cells were washed in ice-cold PBS and then fixed in 80% cold ethanol and stored at 4°C. For flow cytometry analysis, cells were spun down at 100*g* and washed once with PBS containing 0.2% bovine serum albumin. Cell pellets were then resuspended in this washing solution containing 200 μg of RNase A/ml and 100 μg of propidium iodide/ml, and incubated at 37°C for 30 min. DNA fluorescence was measured by flow cytometry using a FACScan Flow fluorescence-activated cell sorter (BD Biosciences Immunocytometry Systems, San Jose, CA), and the percentage of cells in each phase of the cell cycle was determined using Summit software (ver. 3.1; Cytomation, Inc., Fort Collins, CO). Finally, to provide a measure of apoptosis that was independent of DNA fragmentation, in some cases programmed cell death was evaluated by determining caspase activation using the Caspase-Glo 3/7 Assay (Promega Corporation, Madison, WI). These determinations were performed according to the manufacturer's specifications under the same conditions as for the DNA fragmentation ELISA. The enhancement of apoptosis induced by each condition was calculated in relation to control cells that received vehicle alone.

Western Blotting. Total cellular extracts for analysis by Western blotting were prepared in eukaryotic lysis buffer containing protease inhibitors, phosphatase inhibitors, and sample buffer as described previously (Small et al., 2003). These were subjected to Western blotting using standard techniques; immunoreactive protein bands were detected and images acquired and analyzed as in prior studies (Small et al., 2003). The activation status of JNK was determined using rabbit polyclonal or murine monoclonal antibodies recognizing active, dually phosphorylated (Thr183/Tyr185) p54/46 JNK, whereas the status of the p44/42 MAPKs was determined using murine monoclonal antibodies recognizing active, dually phosphorylated ERK-1/2 (Thr202/Tyr204). Activity of the JNK kinase MKK4 was determined using rabbit polyclonal antibodies recognizing active, phosphorylated (Thr261) MKK4 (all from Cell Signaling Technology, Inc., Beverly, MA). Rabbit polyclonal C-19 antibody to MKP-1 was used to evaluate the expression of MKP-1 (Santa Cruz Biotechnology). To provide loading controls, blots were stripped for 45 min using Western Re-Probe (Geno Technology, Inc., St. Louis, MO) following the manufacturer's specifications. They were then reanalyzed with a rabbit polyclonal JNK antibody recognizing the p46 form of JNK (Santa Cruz Biotechnology), or a rabbit polyclonal antibody recognizing both p54 and p46 isoforms (Cell Signaling Technology). As an additional loading control, an antibody recognizing heat shock cognate protein (HSC)-70 was used as well (StressGen Biotechnologies Corp., Victoria, BC, Canada). Horseradish peroxidase-conjugated anti-rabbit and anti-mouse (Amersham Biosciences, Piscataway, NJ) or anti-rat (Santa Cruz Biotechnology) secondary antibodies were used as needed.

JNK Kinase Assays. Adherent cells were seeded onto 60-mm Falcon 3002 tissue culture plates (BD Biosciences Discovery Labware) in complete medium at a density of 2×10^6/plate, allowed to attach overnight, and subjected to conditions described in the text. JNK assays were performed using the SAPK/JNK Assay kit (Cell Signaling Technology), with modifications of the manufacturer's specifications. In brief, cells were washed once with 5 ml of ice-cold PBS and incubated on ice in lysis buffer (consisting of 20 mM Tris-HCl, pH 7.4, 150 mM NaCl, 1 mM EDTA, 1 mM EGTA, 1% Triton X-100, 2.5 mM $Na_4P_2O_7$, 1 mM β-glycerophosphate, 1 mM Na_3VO_4, 1 nM deltamethrin, 180 nM nodularin, 100 μg/ml PMSF, 25 μg/ml aprotinin, 25 μg/ml leupeptin, and 25 μg/ml pepstatin), and scraped (Costar Corporation, Cambridge, MA) into microcentrifuge tubes. Extracts were prepared by sonicating each sample on ice (Heat Systems-Ultrasonics, Inc., Farmingdale, NY), and insoluble material

was removed by microcentrifugation. Relative protein concentrations were determined using the BCA protein assay kit (Pierce Chemical, Rockford, IL), and to equivalent protein amounts corrected for total volume with lysis buffer, 2 μg of glutathione *S*-transferase-c-Jun(1–89) agarose beads (Cell Signaling Technology) were added and rotated overnight at 4°C. JNK-c-Jun complexes were collected and washed with lysis buffer followed by kinase buffer, consisting of 25 mM Tris-HCl, pH 7.5, 5 mM β-glycerophosphate, 2 mM Cleland's reagent, 0.1 mM Na_3VO_4, and 10 mM $MgCl_2$. The in vitro kinase reaction was initiated by addition of kinase buffer containing 100 μM ATP, samples were incubated at 30°C for 45 min, and reactions were terminated by the addition of SDS sample buffer and heating to 95°C for 5 min. Phosphorylated c-Jun was detected by Western blotting using a phosphospecific c-Jun antibody (Cell Signaling Technology).

Xenograft Modeling. All experiments were performed under a protocol approved by the University of North Carolina at Chapel Hill's Institutional Animal Care and Use Committee; where indicated, animals were euthanized by carbon dioxide inhalation using guidelines established by the American Veterinary Medical Association's Panel on Euthanasia. BT-474 cells free of infection with *Mycoplasma* sp. were injected subcutaneously in the flanks of immunodeficient *nu/nu* mice (Charles River Laboratories, Wilmington, MA), and tumor weights were determined thrice weekly as described previously (Somasundaram et al., 2002). When tumors of 100 mg developed, animals were randomized to receive twice-weekly tail vein injections of either vehicle, PS-341 at 1 mg/kg, liposomal doxorubicin at 2 mg/kg, both diluted in PBS, or the combination. Tumor weights were then determined five times weekly by a member of the group who was blinded to the treatment assignments of each cohort.

Statistical Analyses. Paired, two-tailed *t* tests were performed to study the statistical significance of the apoptosis data generated under the conditions described in the text using Prism software (ver. 2.0; GraphPad Software, San Diego, CA). Findings were considered significant if the *p* values were <0.05. For analysis of the xenograft data, a method known as the simple loop analysis (Robertson et al., 1988) was used to examine order-restricted properties of these four drug compound groups. In the nonparametric version of this type of analysis, the null hypothesis is that the mean of the ranks are the same in all four of the groups. The alternative hypothesis is that the mean of the ranks in the control is strictly greater than both of the means of the ranks in the single agent groups, which are strictly greater than the mean of the ranks in the combination group. Therefore, a significant *p*-value in this test gives evidence for this ordering. All *p*-values reported have been adjusted using the Bonferroni method to account for multiple comparisons. Statistical analyses of the data were performed using SAS statistical software (ver. 8.2; SAS Institute Inc., Cary, NC).

Immunohistochemistry. In a separate cohort of animals randomized to the interventions indicated above, 24 h after each treatment, subjects were euthanized using guidelines established by the American Veterinary Medical Association's Panel on Euthanasia. Tumors were excised, fixed, and analyzed as previously noted for apoptosis and phospho-JNK (Somasundaram et al., 2002) as well as for MKP-1 (Small et al., 2003).

Results

MKP-1 Suppresses Proteasome Inhibitor-Mediated Apoptosis. To evaluate the impact of MKP-1 on proteasome inhibitor-mediated apoptosis, A1N4-*myc* human mammary epithelial cells transformed with the *c-myc* oncogene were studied. A1N4-*myc* cells, which require viral-mediated gene delivery, were infected with Ad-GFP/MKP-1 or with Ad-GFP as a control. They were then treated with PS-341 at 10 nM for 18 h, and the extent of apoptosis was quantified using a DNA fragmentation ELISA. Adenoviral infection itself induced a low level of programmed cell death in A1N4-*myc* cells that was equivalent for the two constructs (data not shown). PS-341 induced a 10.7 $\pm$ 1.5-fold increase in apoptosis in Ad-GFP-infected cells (Fig. 1A), but in Ad-GFP/MKP-1-infected cells, this increase was only 6.7 $\pm$ 1.0-fold, consistent with a 37% inhibition of cell death by MKP-1. To verify this finding, the structurally distinct agent Z-LLF-CHO was used; like PS-341, it targets the chymotrypsin-like activity of the proteasome and was the first proteasome inhibitor shown to have antitumor activity in vivo (Orlowski et al., 1998). Here again, proteasome inhibition, this time with 2 μM Z-LLF-CHO for 18 h, induced apoptosis in both Ad-GFP- and Ad-GFP/MKP-1-infected cells (Fig. 1B), but overexpression of MKP-1 inhibited this process by 74%, and for both proteasome inhibitors, these differences were statistically significant ($p = 0.02$).

BT-474-based cell lines stably harboring pcDNA3 or pcDNA3-MKP-1 were constructed and compared as another model system. Treatment with PS-341 increased programmed cell death by 2.6 $\pm$ 0.1-fold in BT-474/pcDNA3 cells (Fig. 1C) but did so by only 1.9 $\pm$ 0.1-fold in BT-474/pcDNA3-MKP-1 cells, consistent with a 27% inhibition of cell death by MKP-1 overexpression. When Z-LLF-CHO was studied, this proteasome inhibitor enhanced cell death by 3.8 $\pm$ 0.2-fold in BT-474/pcDNA3 cells (Fig. 1D) but only by 2.5 $\pm$ 0.2-fold in the BT-474/pcDNA3-MKP-1 cells. This represented a 34% decrease in apoptosis, and for both proteasome inhibitors, this was statistically significant ($p = 0.04$). Because the magnitude of this inhibition was smaller in the stable cell lines; however, we considered the possibility that this could be caused by a lower level of MKP-1 overexpression. Western blotting did indeed indicate that Ad-GFP/MKP-1-infected A1N4-*myc* cells, as well as BT-474/Ad-GFP/MKP-1 cells, expressed a higher level of MKP-1 than BT-474/pcDNA3-MKP-1 cells (data not shown). The impact of this higher level MKP-1 expression on PS-341- and Z-LLF-CHO-induced apoptosis was therefore studied in BT-474 cells. Infection with Ad-GFP/MKP-1 inhibited apoptosis by 67% (Fig. 1E) and 55% (Fig. 1F) ($p = 0.0008$), respectively, compared with Ad-GFP controls, showing a correlation between the level of expression of MKP-1 and the extent of inhibition of programmed cell death.

Suppression of MKP-1 Enhances Proteasome Inhibitor-Mediated Apoptosis. If MKP-1 induction by proteasome inhibitors is indeed antiapoptotic, then down-regulation or deletion of MKP-1 should enhance the sensitivity of cells to this class of drugs. Because pharmacologic agents specifically targeting MKP-1 are not available, BT-474/siMKP-1 cells stably expressing a small interfering RNA that inhibited MKP-1 expression were prepared, along with BT-474/ssMKP-1 cells expressing a scrambled sequence RNA control (Small et al., 2003). The siMKP-1 construct was able to suppress basal levels of MKP-1 expression under control conditions compared with ssMKP-1 (Fig. 2A) and also inhibited the ability of PS-341 to induce MKP-1. At baseline, both of these cell lines had comparable levels of programmed cell death and both were induced to undergo apoptosis by PS-341 (Fig. 2B). Although this proteasome inhibitor increased cell death by 1.5 $\pm$ 0.2-fold in BT-474/ssMKP-1 cells, it did so by 2.5 $\pm$ 0.5-fold in BT-474/siMKP-1 cells, consistent with a 67% increase in sensitivity. When Z-LLF-CHO was used, apoptosis in BT-474/ssMKP-1 cells increased by 5.1 $\pm$ 1.4-fold (Fig.

2C), whereas in BT-474/siMKP-1 cells, this was enhanced by 6.5 ± 2.0-fold ($p = 0.02$ for both). Control experiments showed that antibody-mediated ligation of the Fas receptor in BT-474/siMKP-1 and BT-474/ssMKP-1 cells resulted in comparable levels of cell death (data not shown), indicating that the siMKP-1 construct did not itself affect the cellular apoptotic machinery.

Although inhibition of MKP-1 had enhanced programmed cell death, our siRNA constructs could not completely suppress MKP-1 expression, and we therefore considered the possibility that complete abrogation of this phosphatase would further sensitize cells to proteasome inhibitors. To test this hypothesis, MEFs from MKP-1 knockout (−/−) mice were compared with wild-type (+/+) controls. MKP-1 +/+ MEFs treated with PS-341 demonstrated a 1.4 ± 0.6-fold increase in apoptosis (Fig. 2B), but the increase in MKP-1 −/− cells was 6.9 ± 1.6-fold, or almost 400% greater. When Z-LLF-CHO was tested, apoptosis in MKP-1 +/+ MEFs increased by 2.6 ± 0.4-fold (Fig. 2E), whereas in the −/− MEFs, this occurred by 8.4 ± 1.7-fold, or an almost 225% increase; both values were statistically significant ($p = 0.0001$). Thus, complete deletion of MKP-1 seemed to have a quantitatively greater impact in enhancing apoptosis caused by proteasome inhibitors than did partial MKP-1 inhibition with an siRNA. Taken together, these two sets of studies strongly support the hypothesis that MKP-1 is a mediator of inducible chemoresistance for proteasome inhibitors.

JNK Activations Status Correlates with the Impact of MKP-1 on Apoptosis. Activation of JNK is an important mechanism by which proteasome inhibitors induce apoptosis (Meriin et al., 1998; Hideshima et al., 2003; Yang et al., 2004), and because MKP-1 can dephosphorylate JNK (Kelly and Chu, 2000), it was of interest to determine whether MKP-1 levels and apoptosis correlated with JNK activity. A1N4-*myc* and BT-474 cells infected with adenoviral constructs and then treated with PS-341 were therefore evaluated for their content of dually phosphorylated, activated JNK by Western blotting with phosphospecific antibodies. PS-341 activated JNK by up to 4.5-fold in A1N4-*myc*/Ad-GFP cells compared with the vehicle-treated controls (Fig. 3A), but in A1N4-*myc*/Ad-GFP/MKP-1 cells, this activation was blunted to 1.5-fold. Likewise, after infection of BT-474 cells with Ad-GFP, PS-341 enhanced phospho-JNK levels by 8.3-fold but did so only by 4.3-fold in the Ad-GFP/MKP-1 cells (Fig. 3B). Conversely, in cell lines in which MKP-1 expression was decreased, JNK activation was enhanced in the presence

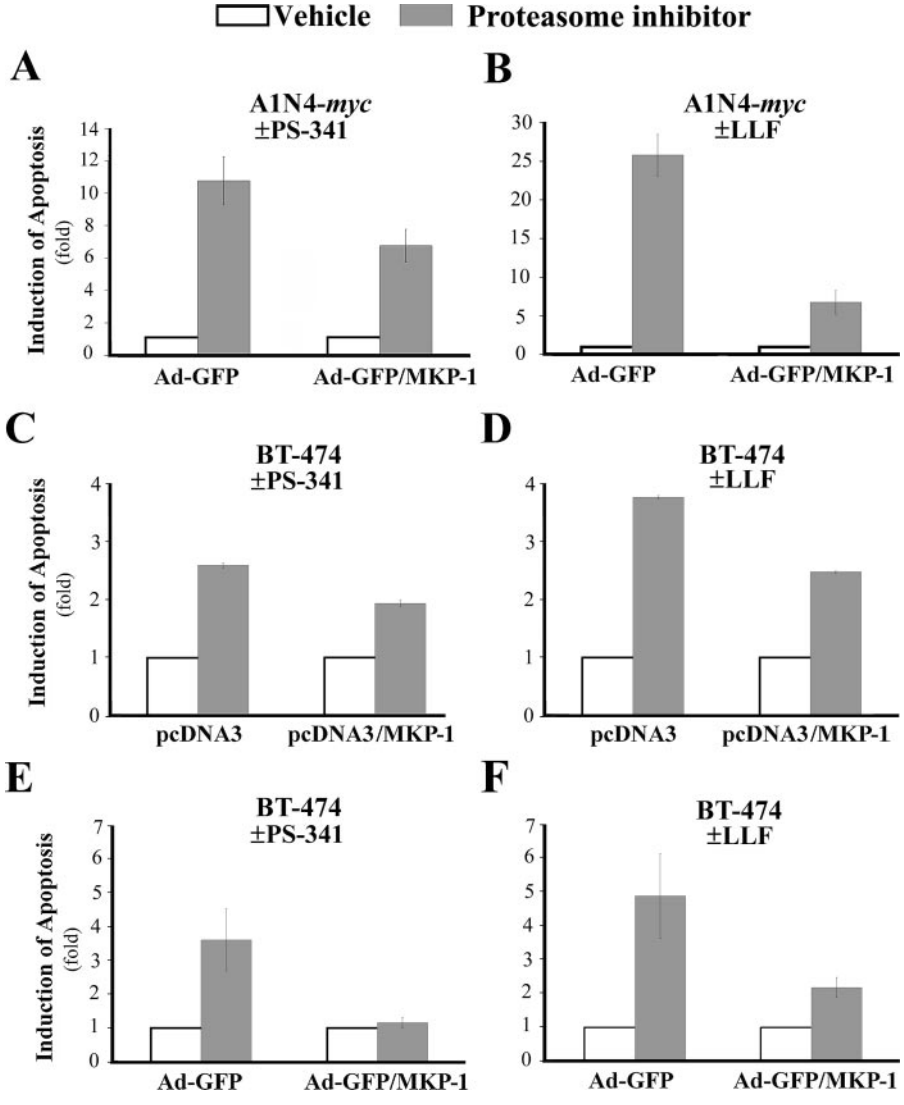

Fig. 1. Effect of MKP-1 on proteasome inhibitor-mediated apoptosis. A, A1N4-*myc* cells were infected with Ad-GFP or Ad-GFP/MKP-1 and 24 h later treated with 10 nM PS-341 for an additional 18 h. Induction of programmed cell death was detected using a DNA fragmentation ELISA, and expressed as a fold-induction over the vehicle controls, which were arbitrarily set at 1.0. The mean is shown, along with the S.E.M., from seven independent experiments. Apoptosis from vehicle is shown in the open bar, whereas apoptosis caused by the proteasome inhibitor is shown in the shaded bar. B, A1N4-*myc* cells infected with Ad-GFP or Ad-GFP/MKP-1 were treated with 2 μM of Z-LLF-CHO (LLF) for 18 h. The mean fold increase in apoptosis ± S.E.M. of four independent experiments is shown. C, BT-474/pcDNA3 control cells and BT-474/pcDNA3/MKP-1 cells were exposed to PS-341 and analyzed as above. The mean ± S.E.M. of seven independent experiments is shown. D, BT-474/pcDNA3 and BT-474/pcDNA3/MKP-1 cells were treated with Z-LLF-CHO and evaluated as above, and the mean ± S.E.M. of seven independent experiments is shown. E, BT-474 cells were infected with Ad-GFP or Ad-GFP/MKP-1 and then treated with vehicle or PS-341 under the same conditions as in C. Apoptosis was evaluated using both a DNA fragmentation ELISA and a caspase-3/7 activity assay; the latter results were shown here after analysis as above, along with the mean ± S.E.M. from 8 independent experiments. F, BT-474 cells were infected with adenoviral vectors and then treated with vehicle or Z-LLF-CHO as in D. The mean induction of apoptosis evaluated by a caspase-3/7 activity assay is shown ± S.E.M. from eight independent experiments.

of a proteasome inhibitor. In BT-474/ssMKP-1 control cells, PS-341 activated JNK by 1.4-fold (Fig. 3C), whereas in BT-474/siMKP-1 cells, this activation occurred by up to 3.3-fold. Finally, in MKP-1 +/+ MEFs, PS-341 increased phospho-JNK levels by 1.3-fold (Fig. 3D), whereas in MKP-1 −/− MEFs, which also had a higher activated JNK content at baseline, proteasome inhibition increased this further by 1.7-fold. These results support the possibility that MKP-1 modulates proteasome inhibitor-mediated programmed cell death through effects on the activation status of JNK.

Suppression of MKP-1 with Anthracyclines Enhances Apoptosis in Vitro. Identification of MKP-1 as a mediator of inducible chemoresistance suggested that modulation of MKP-1 function could enhance the pro-apoptotic efficacy of proteasome inhibitors. Because anthracyclines had been reported to down-regulate MKP-1 expression by repressing function of this phosphatase's promoter (Small et al., 2003), we evaluated the combination of these anti-tumor agents with proteasome inhibitors. In A1N4-*myc* cells, PS-341 induced an increase in apoptosis compared with vehicle controls by 2.8 ± 0.1-fold (Fig. 4A), whereas doxorubicin enhanced cell death by 2.7 ± 0.7-fold. The combination, however, resulted in a 7.0 ± 1.1-fold increase, which was greater than that expected from a simple additive effect of the two agents. Substitution of Z-LLF-CHO for PS-341 in combination with doxorubicin provided confirmatory results, with an increase in apoptosis of 1.8 ± 0.2-fold for Z-LLF-CHO (Fig. 4B), 1.1 ± 0.1-fold for doxorubicin, and 6.9 ± 0.9-fold for the combination ($p = 0.0001$ for the combinations compared with any of the single agents). To determine the proportion of cells undergoing cell death, cell cycle analysis using propidium iodide and fluorescence-activated cell sorting (FACS) was performed to identify cells with a sub-G_1 DNA content. At baseline, most cells had at least a diploid DNA content, with only 0.6% of cells undergoing apoptosis (Fig. 4C). Neither PS-341 alone nor doxorubicin alone affected this level significantly, but the combination induced loss of DNA content to sub-G_1 levels, consistent with apoptosis, in 31.1% of cells. To evaluate the effect of combination therapy on MKP-1 and JNK, extracts from A1N4-*myc* cells treated with vehicle, PS-341, doxorubicin, or both, were probed by Western blotting. JNK activation, as reflected by the levels of the dually phosphorylated JNK kinases, was induced with doxorubicin up to 2.6-fold (Fig. 4D) and with PS-341 up to 3.0-fold, but the combination enhanced phospho-JNK by up to 9.3-fold. This was associated with a suppression of MKP-1 expression in the doxorubicin/PS-341 combination to levels below that seen with PS-341 as a single agent and indeed to levels comparable with those seen with vehicle treatment alone. A direct measure of kinase activity was also obtained by precipitation of JNK with a c-Jun fusion protein followed by an in vitro kinase assay, after which the phospho-c-Jun product was detected by Western blotting. Proteasome inhibition with Z-LLF-CHO activated JNK by 5.2-fold (Fig. 4E), doxorubicin

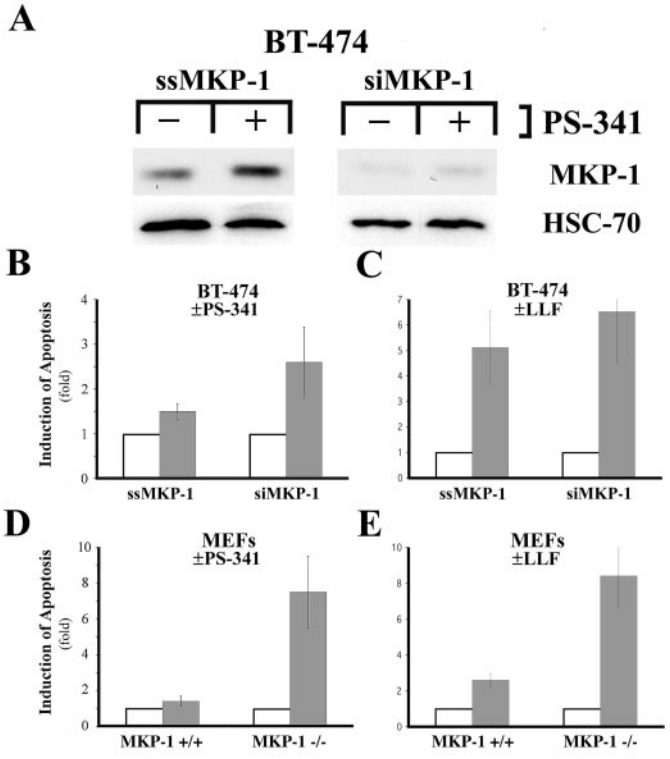

Fig. 2. Suppression of MKP-1 and proteasome inhibitor-mediated apoptosis. A, BT-474/ssMKP-1 control cells and BT-474/siMKP-1 cells stably expressing an siRNA to MKP-1 were constructed as described previously (Small et al., 2003). During the process of screening colonies, their MKP-1 expression was studied by treating with either vehicle (−) or with 5 nM PS-341 for 4 h, followed by Western blotting of protein extracts. B, BT-474/ssMKP-1 and BT-474/siMKP-1 cells were treated with 10 nM PS-341 for 18 h, and apoptosis was analyzed by a DNA fragmentation assay. The mean ± S.E.M. of nine independent experiments is shown. C, BT-474/ssMKP-1 and BT-474/siMKP-1 cells were treated with 2 μM Z-LLF-CHO, apoptosis was analyzed as above, and the mean ± S.E.M. of eight independent experiments is shown. D, wild-type MKP-1 +/+ MEFs and MKP-1 knockout −/− MEFs were treated with 5 nM PS-341 for 18 h, apoptosis was analyzed as above, and the mean ± S.E.M. of five independent experiments is shown. E, MKP-1 +/+ and −/− MEFs were treated with 2 μM Z-LLF-CHO for 18 h, apoptosis was analyzed as above, and the mean ± S.E.M. of five independent experiments is shown.

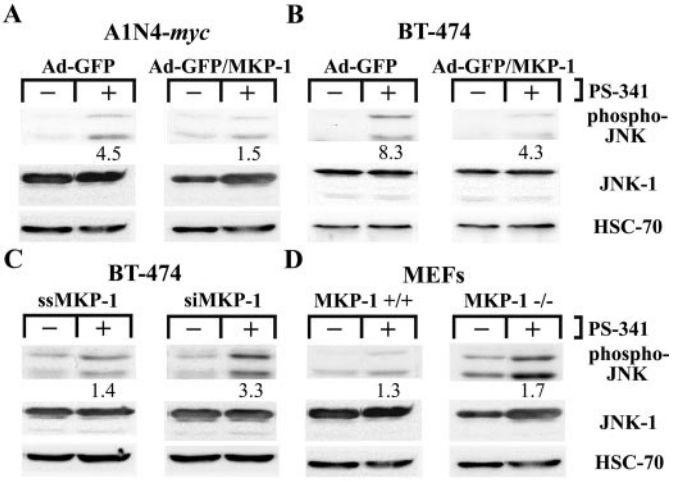

Fig. 3. MKP-1 and phospho-JNK levels. A, A1N4-*myc* cells infected and treated as described previously were analyzed for phospho-JNK content by Western blotting with a phosphospecific JNK antibody that recognized dually phosphorylated activated JNK-1 and -2. The blots were then stripped and reprobed with an antibody recognizing JNK-1 in a phosphorylation state-independent manner and then with an antibody recognizing HSC-70 as a loading control. The fold increase in phospho-JNK content as a result of proteasome inhibition is shown compared with the relevant vehicle control, and adjusted for loading of JNK-1. The data are representative of two experiments. B, BT-474 cells infected with Ad-GFP or Ad-GFP/MKP-1 were treated with PS-341 and analyzed for phospho-JNK. C, BT-474/ssMKP-1 and BT-474/siMKP-1 cells were treated with PS-341 and analyzed as above. D, wild-type MKP-1 +/+ MEFs and knockout −/− MEFs were treated and analyzed as above.

did so by up to 2.6-fold, but the combination increased JNK activity by up to 29.6-fold.

To evaluate the response of BT-474 cells to the proteasome inhibitor/anthracycline regimen, they were treated with either PS-341 or Z-LLF-CHO and doxorubicin. PS-341 induced a 1.5 ± 0.2-fold increase in apoptosis (Fig. 5A), doxorubicin did so by 2.0 ± 0.5-fold, and the combination accomplished a 5.7 ± 0.8-fold increase, whereas for Z-LLF-CHO and doxorubicin, the comparable results were 1.6 ± 0.2- (Fig. 5B), 1.5 ± 0.2-, and 11.2 ± 4.0-fold, respectively ($p = 0.003$ for both combinations compared with any of the single agents). Cellular death was also evaluated by cell cycle analysis; again, at baseline, few cells were apoptotic (Fig. 5C). Whereas PS-341 induced loss of DNA content in 27.7% of cells, doxorubicin did so in 3.5%, and the combination accomplished this in 64.7%. Analysis of phospho-JNK levels showed that PS-341 induced JNK by up to 2.4-fold (Fig. 5D), doxorubicin did so by up to 5.0-fold, and the combination accomplished a 33.0-fold increase. This was accompanied by a suppression of MKP-1 protein to expression levels that were much lower than with PS-341 alone and again more reflective of MKP-1 in vehicle-treated BT-474 cells. JNK activity was also enhanced by the Z-LLF-CHO/doxorubicin combination (Fig. 5E) to a greater extent than was the case for either the proteasome inhibitor or the anthracycline as single agents.

It was also of interest to confirm some of these results with

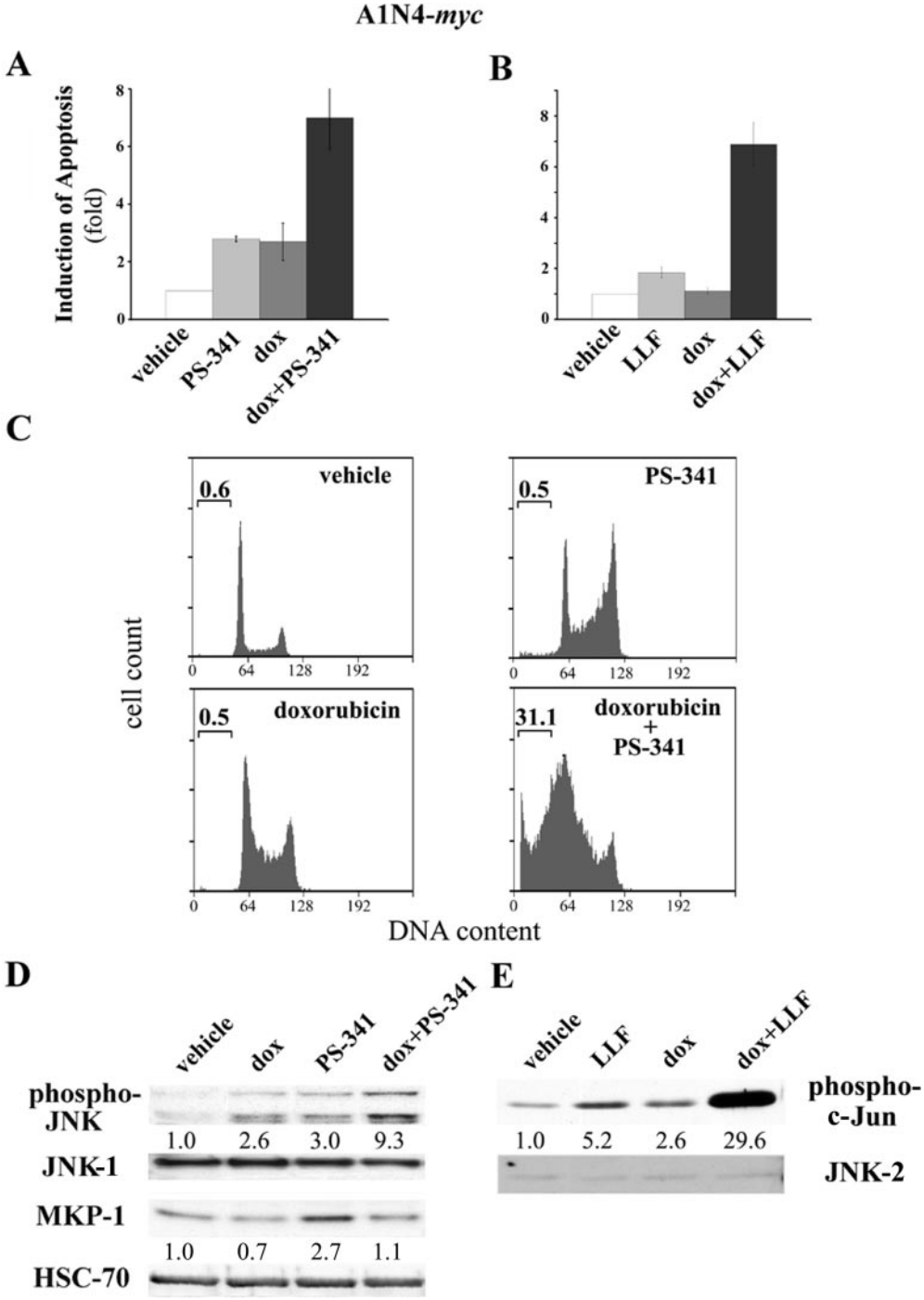

Fig. 4. Impact of the addition of doxorubicin to a proteasome inhibitor in A1N4-*myc* cells. A, A1N4-*myc* cells were treated with vehicle, 5 nM PS-341, 1 μM doxorubicin, or the combination for 18 h. Apoptosis was then evaluated and expressed as a fold-induction over the vehicle control, and the mean ± S.E.M. of eight experiments is shown. B, A1N4-*myc* cells were treated with vehicle, 2 μM Z-LLF-CHO, 5 μM doxorubicin, or the combination for 12 h, and evaluated as described above. The mean ± S.E.M. of four experiments is shown. C, A1N4-*myc* cells were treated as in A, stained with propidium iodide, and DNA content was analyzed by FACS. The percentage of apoptotic cells as determined by those with a sub-G_1 DNA content is shown. These data are representative of two experiments. D, extracts of A1N4-*myc* cells treated as in A were analyzed for phospho-JNK content, as well as JNK-1, MKP-1, and HSC-70. The -fold increase in phospho-JNK content compared with the vehicle control and adjusted for loading of JNK-1 is shown. Induction of MKP-1 is also shown as a fold increase compared with the vehicle control and adjusted for loading of HSC-70. These data are representative of two experiments. E, JNK activity was determined in A1N4-*myc* cells treated as in B by precipitating JNK, followed by an in vitro kinase assay using c-Jun as a substrate. The phospho-c-Jun product was detected by Western blotting, and the fold-induction is shown compared with the vehicle control after adjusting for immunoprecipitation efficiency as determined by reprobing the blot for JNK-2. These data are representative of two experiments.

another anthracycline; therefore, A1N4-*myc* and BT-474 cells were studied with PS-341 and epirubicin. Apoptosis in both of these cell lines was induced by the combination regimen to a greater than additive extent compared with the single agent therapies (Fig. 6, A and B, respectively) ($p = 0.02$ for both). This was associated with similarly enhanced phospho-JNK levels and MKP-1 suppression (Fig. 6C and D, respectively). Taken together, these findings support the hypothesis that the addition of an anthracycline to a proteasome inhibitor results in enhanced induction of programmed cell death and activation of JNK, accompanied by suppression of MKP-1 expression.

An Anthracycline/Proteasome Inhibitor Regimen Has Enhanced Activity in Vivo. The finding that a regimen combining an anthracycline and a proteasome inhibitor resulted in activation of apoptosis to a greater extent than did either agent alone suggested that such a combination could have enhanced antitumor activity in vivo as well. To evaluate this possibility and to allow probing of the hypothesis that this was occurring because of anthracycline-mediated suppression of MKP-1 in vivo, a xenograft model of human breast cancer based on the BT-474 cell line was used. Subjects were randomized to receive twice-weekly injections of vehicle, PS-341 at 1 mg/kg, liposomal doxorubicin at 2 mg/kg, or the combination of the two; both agents were administered on the same day. Using data from a smaller pilot experiment that showed a trend for superiority of the two-agent combination in comparison with either of the two sin-

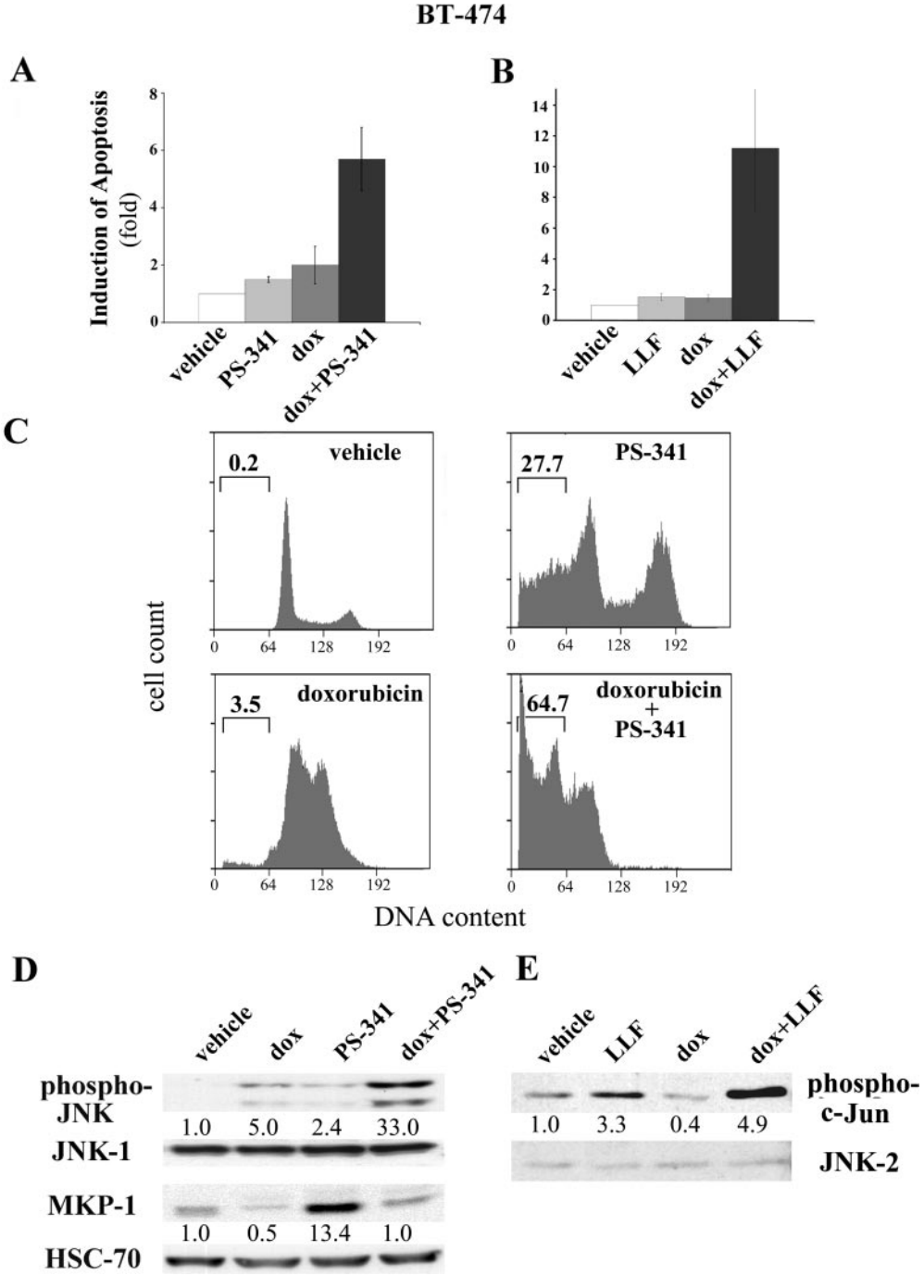

Fig. 5. Impact of the addition of doxorubicin to a proteasome inhibitor in BT-474 cells. A, BT-474 cells were treated with vehicle, 5 nM PS-341, 1 μM doxorubicin, or the combination for 18 h. Apoptosis was then evaluated and expressed as for the experiments in Fig. 4. The mean ± S.E.M. of eight experiments is shown. B, BT-474 cells were treated with vehicle, 2 μM Z-LLF-CHO, 5 μM doxorubicin, or the combination for 12 h and evaluated for apoptosis as described above. The mean ± S.E.M. of eight experiments is shown. C, BT-474 cells were treated as in A, stained with propidium iodide, and their DNA content was analyzed by FACS. The percentage of apoptotic cells with a sub-G_1 DNA content is shown. These data are representative of two experiments. D, extracts of BT-474 cells treated as in A were analyzed for phospho-JNK, JNK-1, MKP-1, and HSC-70. The fold increase in phospho-JNK content and for MKP-1 are shown and were determined as described previously. These data are representative of two experiments. E, JNK activity was determined in BT-474 cells treated as in B by an in vitro kinase assay. The phospho-c-Jun product was then detected by Western blotting, and the fold-induction is shown compared with the vehicle control after adjusting for immunoprecipitation efficiency. These data are representative of two experiments.

gle drugs (data not shown), an effect size was calculated and a second, larger study was performed to confirm these initial findings (Fig. 7). Both PS-341 and doxorubicin had some affect on tumor growth, but there was a trend for the combination to show enhanced tumor growth delay. At day 15, for example, calculated tumor weights were 1793 ± 307 mg in the vehicle-treated group, 1102 ± 145 mg in the doxorubicin-treated group, 1397 ± 228 mg in the PS-341-treated group, and 846 ± 97 mg in the combination group. A priori, there was an interest in the ordering of the tumor size response over the four groups, and this could be exploited by simple loop analysis (Robertson et al., 1988). Using a nonparametric version of this method to test the null hypothesis that the mean ranks of the four groups were equivalent, the scientific hypothesis of interest was that the mean of the ranks in the control was strictly greater than both of the means of the ranks in the single agent groups, which were strictly greater than the mean of the ranks in the combination group. There was significant evidence to support the scientific hypothesis in this data set ($p = 0.03$) and reject the null hypothesis, supporting the superiority of the PS-341 and doxorubicin regimen.

In that the addition of an anthracycline to a proteasome inhibitor induced enhanced apoptosis in vitro in association with suppression of MKP-1 and enhanced phospho-JNK, it was of interest to evaluate whether this also occurred in vivo. Tumor tissue from two separate xenograft cohorts was therefore harvested 24 h after each treatment and analyzed subsequently by immunofluorescence. Both PS-341 and doxorubicin as single agents were able to induce programmed cell death in comparison with vehicle controls (Fig. 8A), but the combination resulted in more apoptosis than either drug alone. With regard to MKP-1, PS-341 induced an increase in expression of this phosphatase above the levels seen at baseline (Fig. 8B), whereas doxorubicin suppressed MKP-1 below the levels seen with the vehicle control. Addition of the anthracycline to PS-341 resulted in an intermediate level of MKP-1 expression that was higher than with doxorubicin alone but lower than that seen with PS-341 or vehicle. Finally, phospho-JNK levels seemed to parallel those of apoptosis (Fig. 8C), with some increase seen in phospho-JNK after treatment with either PS-341 or doxorubicin. The greatest levels of phospho-JNK were seen with the anthracycline/proteasome inhibitor combination, however, and corresponded to the suppression of MKP-1 by doxorubicin. These studies demonstrate that modulation of MKP-1 and phospho-JNK occurs at physiologically relevant doses of the two agents and supports the hypothesis that this contributes to the enhanced apoptosis and antitumor efficacy of the combination.

The Anthracycline/Proteasome Inhibitor Regimen Induces Apoptosis in Part through JNK, Whereas ERK Is Antiapoptotic. Combination therapy with an anthracycline and a proteasome inhibitor seemed to enhance apoptosis and phospho-JNK in association with suppression of MKP-1. To examine more directly whether this apoptosis was occurring through JNK, the effect of modulating JNK function on the ability of the doxorubicin/PS-341 regimen to induce cell death was studied. A1N4-*myc* cells, which could inducibly express c-Jun-TAM-67, a dominant-negative mutant of the JNK downstream effector c-Jun, were prepared. Uninduced A1N4-*myc*/pLRT-c-Jun-TAM-67 cells treated with doxorubicin and PS-341 had an increase in apoptosis by 5.4 ± 0.5-fold (Fig. 9A), but upon induction of DN-c-Jun with doxycycline, this increase was blunted to 3.7 ± 0.7-fold ($p = 0.008$). Doxycycline itself did not affect apoptosis caused by doxorubicin and PS-341 in parental A1N4-*myc* cells or in A1N4-*myc*/pLRT-GFP cells (data not shown). Likewise, in BT-474 cells constitutively expressing c-Jun-TAM-67 from pcDNA3.1, the combination enhanced apoptosis by 13.1 ± 1.1-fold (Fig. 9B) compared with 17.8 ± 1.0-fold in vector control cells. Finally, expression of a dominant-negative JNK-1α also inhibited apoptosis caused by the combination

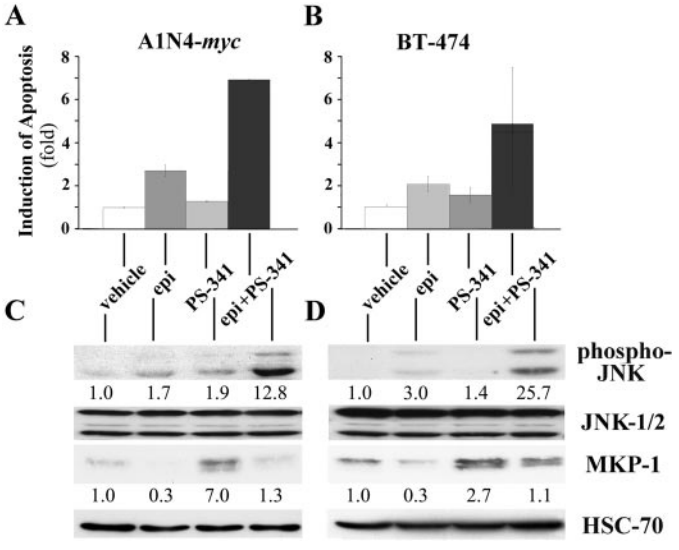

Fig. 6. Impact of the addition of epirubicin to a proteasome inhibitor. A, A1N4-*myc* cells were treated with vehicle, 5 nM PS-341, 1 μM epirubicin, or the combination for 18 h. Apoptosis was then evaluated using a DNA fragmentation ELISA and expressed as a -fold induction of apoptosis over the vehicle control. The mean ± S.E.M. of four experiments is shown. B, BT-474 cells were treated and analyzed as in A above. The mean ± S.E.M. of four experiments is shown. C, extracts of A1N4-*myc* cells treated as in A were analyzed for phospho-JNK, JNK-1/2, MKP-1, and HSC-70. The -fold increase in phospho-JNK and MKP-1 content for each condition is shown. These data are representative of two experiments. D, extracts of BT-474 cells treated as in B were analyzed for phospho-JNK, JNK-1/2, MKP-1, and HSC-70 as above. These data are representative of two experiments.

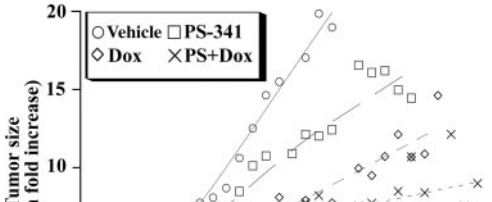

Fig. 7. Efficacy of a proteasome inhibitor/anthracycline regimen in vivo. A xenograft model of human breast carcinoma was developed by subcutaneous injection of BT-474 cells into *nu/nu* mice. These were then randomly assigned to receive twice-weekly injections of vehicle, PS-341 at 1 mg/kg, liposomal doxorubicin at 2 mg/kg, or the combination. Tumor measurements were obtained five times by a member of the team who was blinded to the treatment assignments and were used to calculate tumor weight. The graph shows the mean -fold increase in tumor weight for each group ($n = 15$) with time compared with the first day of vehicle or drug therapy (day 0).

therapy; cell death was induced by only 12.4 ± 0.4-fold (p = 0.009 for both).

Another important target for MKP-1 that can affect apoptosis is p44/42 MAPK, which mediates its effects in part through the downstream effector Bad (Bonni et al., 1999; Scheid et al., 1999). In previous studies, we identified the ability of proteasome inhibitors to suppress p44/42 (Orlowski et al., 2002a) and the action of anthracyclines to stimulate p44/42 (Small et al., 2003); it was therefore of interest to determine the effect of treatment with the combination. Because the net impact of doxorubicin/PS-341 was to suppress MKP-1, it was anticipated that phospho-ERK levels would increase in parallel with phospho-JNK. Western blots of A1N4-*myc* cells showed that ERK-1/2 was activated by up to 2.5-fold (Fig. 9C), whereas in BT-474, this occurred by up to 2.1-fold (Fig. 9D), as judged by the levels of the dually phosphorylated activated kinases. To examine the effect of this ERK activation on cell death, A1N4-*myc* cells expressing either vector sequences or a dominant-positive ERK-2 mutant were treated with doxorubicin/PS-341. In A1N4-*myc*/pLPCX cells, apoptosis was induced by 5.8 ± 1.2-fold (Fig. 9E), whereas in A1N4-*myc*/pLPCX-DP-ERK-2 cells, the combination enhanced cell death by only 2.0 ± 0.7-fold. Likewise, in BT-474 cells, doxorubicin/PS-341 enhanced apoptosis by 12.1 ± 4.3-fold (Fig. 9F), but in BT-474/DP-ERK-1/2 cells, this occurred to only 6.4 ± 0.7-fold (p = 0.03 for both). Together, these findings support the hypothesis that the anthracycline/proteasome inhibitor regimen results in increased activation of apoptosis through the JNK pathway, but that its own activity is limited by enhanced activation of ERK because of suppression of MKP-1.

MKP-1 Is Directly Involved in the Mechanism of Action of the Anthracycline/Proteasome Inhibitor Combination. Although the ability of doxorubicin to suppress MKP-1 in both cell and in vivo models supported the possibility that this led to enhanced JNK activation and apoptosis, the anthracycline/proteasome inhibitor combination may interact through a number of mechanisms. Anthracyclines, for example, activate NF-κB, whereas proteasome inhibitors block this activation, and because NF-κB is antiapoptotic through its induction of members of the Bcl-2 and inhibitor of apoptosis families (Voorhees et al., 2003), this mechanism could account for the enhanced anti-tumor efficacy of the combination regimen. Therefore, to more directly evaluate the role of MKP-1, advantage was taken of the finding that anthracyclines specifically repressed MKP-1 promoter function while sparing the CMV immediate early region promoter (Small et al., 2003). A1N4-*myc* cells were therefore infected either with Ad-GFP or Ad-GFP/MKP-1 and then treated either with vehicle, doxorubicin, PS-341, or the combination. As expected, overexpression of GFP did not affect the ability of the proteasome inhibitor/anthracycline combination to induce increased levels of apoptosis (Fig. 10A) and to enhance phospho-JNK while suppressing MKP-1 (Fig. 10B). Forced overexpression of MKP-1, however, which had a negligible effect on doxorubicin-mediated cell death (Fig. 10A), inhibited PS-341-induced apoptosis and also prevented the ability of the combination from resulting in enhanced programmed cell death (p = 0.01). This was associated with a decrease in JNK activation, as reflected in the levels of the dually phosphorylated kinase (Fig. 10B). As a further test of our hypothesis, BT-474/ssMKP-1 and BT-474/siMKP-1 cells were compared in a similar fashion. In the control BT-474/ssMKP-1 cells, the anthracycline/proteasome inhibitor regimen did result in enhanced apoptosis (Fig. 10C), along with increased JNK activation and suppression of MKP-1 (Fig. 10D). In BT-474/siMKP-1 cells, however, where MKP-1 was suppressed further by a specific siRNA, the doxorubicin/PS-341 combination induced a higher level of apoptosis (p = 0.02) and JNK activation than in the BT-474/ssMKP-1 controls. Although the anthracycline/proteasome inhibitor combination may interact in several ways to enhance apoptosis, therefore, suppression of MKP-1 is an important part of the mechanism of action of this novel regimen.

Discussion

Many chemotherapeutic agents have pleiotropic effects, and although on balance they activate programmed cell death, they may also induce antiapoptotic pathways that

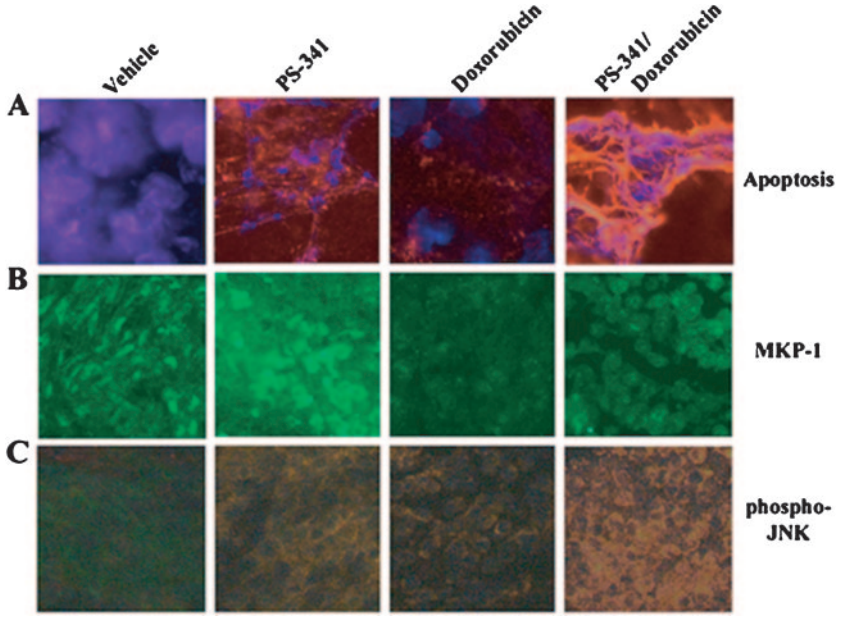

Fig. 8. Apoptosis, MKP-1, and phospho-JNK in xenograft tumor tissue. A, tumor tissue was harvested from a separate xenograft cohort 24 h after each of the indicated treatments, and subsequently analyzed by immunofluorescence. To evaluate for the induction of apoptosis, sections were probed for the presence of single-stranded sequences after formamide-induced DNA denaturation using a murine monoclonal antibody. The background blue staining in all panels is a 4,6-diamidino-2-phenylindole nuclear stain, whereas apoptosis is seen in red. B, expression of MKP-1 was evaluated using a rabbit polyclonal antibody; green staining indicates the presence of MKP-1. C, the activation state of JNK was probed by dual staining with a murine monoclonal antibody recognizing the phosphorylated, activated form of JNK, and a rabbit polyclonal antibody recognizing JNK in a phosphorylation status-independent manner. Nuclei were also stained with 4,6-diamidino-2-phenylindole as above, and separate images taken with appropriate filters were fused together. Nonphosphorylated JNK is seen in green, whereas phosphorylated JNK appears as an orange-brown color in this overlay.

promote tumor survival. The proteasome is an attractive target for cancer therapy (Voorhees et al., 2003), and PS-341 (bortezomib; Adams et al., 1999), the first proteasome inhibitor to enter clinical trials, has recently been approved by the Food and Drug Administration for patients with multiple myeloma who have received at least two prior therapies and progressed on the last of these, and is being investigated in other tumor types as well, including breast cancer (Orlowski and Dees, 2003). A better understanding of the molecular mechanisms of action of such agents will aid in their optimal clinical application. Moreover, identification of antiapoptotic activities of proteasome inhibitors could lead to the design of novel, rational combination regimens with the promise of enhanced anti-tumor efficacy.

Proteasome inhibitors induce apoptosis in part through JNK activation (Meriin et al., 1998; Hideshima et al., 2003; Yang et al., 2004), but also transcriptionally induce MKP-1

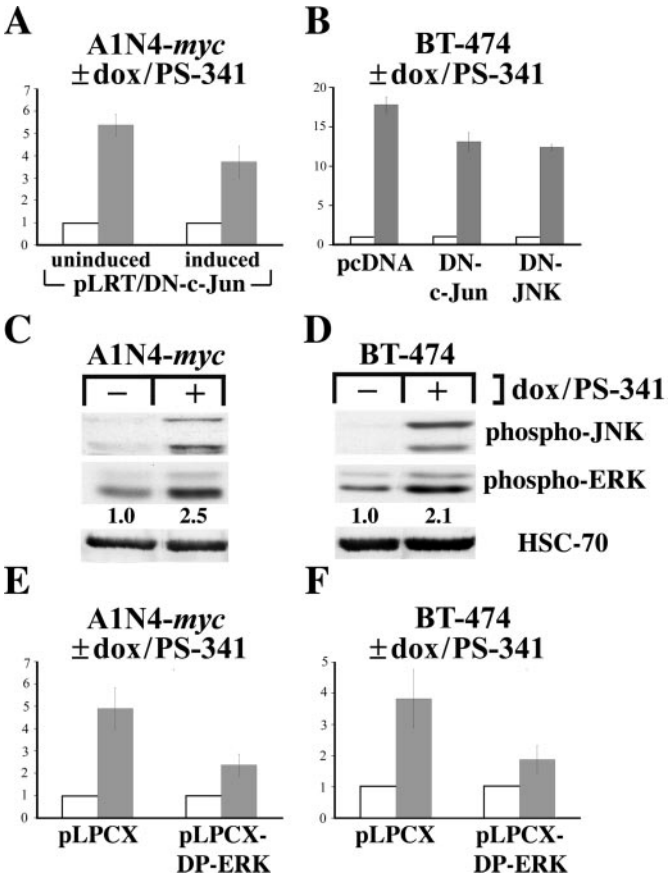

Fig. 9. The role of ERK and JNK in apoptosis as a result of the doxorubicin/PS-341 regimen. A, A1N4-*myc* cells harboring pLRT-c-Jun-TAM-67 were induced with doxycycline at 10 μg/ml for 24 h, and then treated with the doxorubicin and PS-341 as described in the legend to Fig. 4. Apoptosis was evaluated by DNA fragmentation and confirmed with caspase-3/7 assays, and the latter results are shown here as the mean -fold induction of caspase activity over the uninduced vehicle control, which was set at 1.0 ± S.E.M. from four independent experiments. B, BT-474 cells harboring pcDNA, pcDNA/c-Jun-TAM-67, or pcDNA/DN-JNK-1α were treated with doxorubicin and PS-341 under the conditions described in the legend to Fig. 4. Apoptosis was evaluated by DNA fragmentation and confirmed with caspase-3/7 assays, and the latter results are shown here as the mean -fold induction of caspase activity ± S.E.M. from four independent experiments. C, A1N4-*myc* cells treated with doxorubicin and PS-341 as described above were subjected to Western blotting to detect the expression levels of the dually phosphorylated activated JNK-1/2. They were then stripped and reprobed with an antibody recognizing dually phosphorylated activated ERK-1/2. To confirm loading, they were stripped and reprobed with an antibody recognizing HSC-70. C and D show representative results from one of two independent experiments. The -fold activation of ERK-1/2 by the combination of doxorubicin and PS-341 is shown in relation to vehicle-treated controls, which were arbitrarily set at 1.0, after correction for loading of HSC-70. D, BT-474 cells treated with doxorubicin and PS-341 as above were analyzed for activated JNK-1/2, activated ERK-1/2, and HSC-70. E, A1N4-*myc* cells harboring pLPCX or pLPCX/DP-ERK-2 were treated with doxorubicin and PS-341, analyzed by DNA fragmentation, and the mean -fold induction of apoptosis over the vehicle control is shown ± S.E.M. from four independent experiments. F, BT-474 cells harboring either pLPCX or pLPCX/DP-ERK-1/-2 were treated and analyzed as above, and the mean fold-induction of apoptosis over the vehicle control is shown ± S.E.M. from four independent experiments.

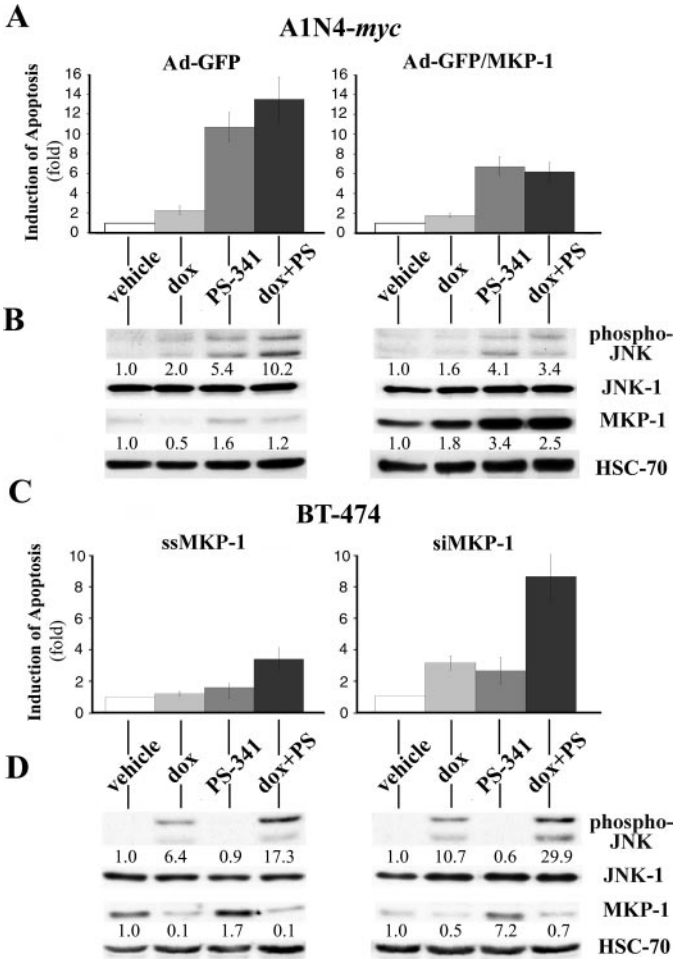

Fig. 10. The role of MKP-1 in the doxorubicin/PS-341 regimen. A, A1N4-*myc* cells were infected with Ad-GFP or Ad-GFP/MKP-1 and treated with vehicle, 5 nM PS-341, 1 μM doxorubicin, or the combination for 18 h. Apoptosis was evaluated using a DNA fragmentation ELISA and expressed as a fold-induction of apoptosis over the vehicle control ± S.E.M. from seven independent experiments. B, extracts from A1N4-*myc* cells treated as in A were analyzed for phospho-JNK, MKP-1, and JNK-1. The fold increase in phospho-JNK content for each condition compared with the vehicle control, and adjusted for loading as above, is shown. MKP-1 expression is shown to document the overexpression induced with the Ad-GFP/MKP-1 construct. These data are representative of two experiments. C, BT-474/ssMKP-1 and BT-474/siMKP-1 cells were treated with vehicle, 5 nM PS-341, 1 μM doxorubicin, or the combination for 18 h. Apoptosis was then evaluated using a DNA fragmentation ELISA and expressed as a -fold induction of apoptosis over the vehicle control ± S.E.M. from four independent experiments. D, extracts from BT-474/ssMKP-1 and BT-474/siMKP-1 cells treated as in C were analyzed for phospho-JNK, MKP-1, and JNK-1. The fold increase in phospho-JNK and MKP-1 content is shown. Although the fold induction of MKP-1 by PS-341 is greater in the BT-474/siMKP-1 cells, this is caused by the lower basal levels of MKP-1, and relative MKP-1 content is still lower than in BT-474/ssMKP-1 cells. These data are representative of two experiments.

(Orlowski et al., 2002a). Given the ability of MKP-1 to inhibit JNK (Kelly and Chu, 2000), we considered the possibility that the induction of this phosphatase might suppress proteasome inhibitor-mediated cell death. In the studies presented herein, we found that overexpression of MKP-1 protected transformed human mammary epithelial and breast carcinoma cells from apoptosis caused by two structurally distinct proteasome inhibitors (Fig. 1), and the extent of over-expression seemed to correlate with the amount of suppression of cell death. Conversely, MKP-1 suppression resulted in enhanced sensitivity to proteasome inhibitors (Fig. 2), whereas its complete deletion further increased the ability of proteasome inhibitors to induce apoptosis. Enhanced expression of MKP-1 in the setting of suppressed apoptosis was associated with decreased levels of phospho-JNK (Fig. 3). Conversely, when MKP-1 was either specifically suppressed or inactivated, increased apoptosis correlated with enhanced phospho-JNK levels. These findings support the hypothesis that MKP-1 is a mediator of inducible chemoresistance to proteasome inhibitors and that it functions, at least in part, by inhibiting JNK activity.

MKP-1 is a part of the heat shock and stress response pathways, and it is interesting to note that both heat shock protein (HSP)-70 as well as HSP-27 have been reported to mediate resistance to proteasome inhibitors. HSP-70 activation, in analogy with MKP-1, was shown to interfere with induction of JNK (Meriin et al., 1998; Robertson et al., 1999), whereas HSP-27 worked in part by blocking release of second mitochondria-derived activator of caspases (Chauhan et al., 2003a,b). Moreover, recent studies have shown that inhibition of HSP-90 can potentiate the efficacy of proteasome inhibitors (Mimnaugh et al., 2004). These findings indicate that several of the major HSP families are involved in protecting cells from the proapoptotic effects of drugs such as PS-341. Patients who are being considered candidates for therapy with a proteasome inhibitor may therefore eventually benefit from an evaluation of the activation status of these HSPs, either through a gene array analysis, proteomic analysis, or both. Once specific agents targeting each individual family are available, such patients could be directed toward combination regimens designed to inhibit the HSP most activated in their disease, along with a proteasome inhibitor.

The antiapoptotic effects of MKP-1 suggested that pharmacologic inhibition of its induction could enhance the ability of proteasome inhibitors to activate programmed cell death. Because specific inhibitors of MKP-1 are not yet available and anthracyclines repressed MKP-1 promoter function (Small et al., 2003), we considered the possibility that a proteasome inhibitor/anthracycline regimen would induce enhanced apoptosis. Combinations incorporating a proteasome inhibitor and an anthracycline indeed resulted in a greater than additive activation of programmed cell death in vitro (Figs. 4–6), and antitumor activity in vivo (Fig. 7). Previous reports have documented synergy between these two classes of drugs in models of myelogenous leukemia (Guzman et al., 2002) and multiple myeloma in vitro (Ma et al., 2003; Mitsiades et al., 2003). The current findings represent the first data on the combination in breast cancer, however, and also the first documentation in any model that the combination has enhanced activity in vivo. Together, these results strongly support clinical testing of such regimens and, in part, motivated the design of a recently completed phase I study of a combination of bortezomib with pegylated, liposomal doxorubicin at our institution. This regimen was well tolerated, resulted in documented clinical benefit in patients with solid tumors, including breast cancer, and with hematologic malignancies, such as multiple myeloma (Voorhees et al., 2003). Further phase II testing in both patient populations is planned.

Combination regimens including an anthracycline and a proteasome inhibitor probably cooperate to enhance their proapoptotic effects and antitumor efficacy through a number of molecular mechanisms that do not involve MKP-1. The ability of proteasome inhibitors to abrogate anthracycline-mediated activation of antiapoptotic NF-κB is certainly one of these (Ma et al., 2003; Mitsiades et al., 2003; Voorhees et al., 2003). Another possibility that has been strongly implicated is the suppression of DNA damage repair proteins by proteasome inhibitors (Mitsiades et al., 2003). This may make cells more susceptible to DNA damaging agents such as anthracyclines, which work through a number of mechanisms relevant to this hypothesis, including inhibiting topoisomerase II, generating oxygen free radicals, and intercalating into DNA (Riggs, 1997). We therefore wished to verify that repression of MKP-1 contributed, at least in part, to these other mechanisms. For both A1N4-*myc* and BT-474 cells, the addition of an anthracycline to a proteasome inhibitor enhanced phospho-JNK levels (Figs. 4–6) and JNK activity (Figs. 4, 5) while suppressing MKP-1 (Figs. 4–6). In addition, in A1N4-*myc* cells, these combinations did not activate the JNK kinase MKK4, as determined by levels of the phosphorylated activated protein, suggesting that the enhanced phospho-JNK levels were not caused by increased activity of the upstream kinases (data not shown). However, in BT-474 cells, mild MKK4 activation was occasionally seen, possibly indicating some cell-type specificity but also the need for a more direct approach. Therefore, forced overexpression of MKP-1 from a CMV promoter that was not anthracycline-suppressible (Small et al., 2003) was pursued, and this abrogated the ability of the combination to enhance apoptosis and phospho-JNK expression (Fig. 10A). Conversely, further suppression of MKP-1 with an siRNA in BT-474 cells enhanced apoptosis and phospho-JNK caused by the combination compared with controls (Fig. 10B). These findings support the hypothesis that suppression of MKP-1 is one mechanism by which anthracyclines enhance proteasome inhibitor-mediated programmed cell death and suggest that targeting MKP-1 is one strategy for chemosensitization to proteasome inhibitors.

Several factors contribute to the induction of MKP-1, including activation of both p44/42 and p38 MAPKs (Camps et al., 2000; Li et al., 2001). Inhibition of MKP-1 through p44/42 or p38 pathway blockade may therefore be alternative mechanisms to the use of anthracyclines to suppress MKP-1 and enhance apoptosis. In this regard, previous studies with proteasome inhibitor-based combinations incorporating a p44/42 MAPK kinase (MEK) inhibitor (Orlowski et al., 2002a) or a p38 inhibitor (Meriin et al., 1998) have reported enhanced programmed cell death. It would therefore be of interest to evaluate the extent to which these regimens impact upon MKP-1 and to evaluate these regimens in vivo. The finding that the pro-apoptotic activity of the anthracycline/proteasome inhibitor regimen is itself limited by increased activa-

tion of ERK highlights the pleiotropic nature of MKP-1, which has both pro-apoptotic activities through inhibition of p44/42 MAPK signaling, and antiapoptotic activities through suppression of JNK. For the mammary epithelial and breast carcinoma model systems used in our work, the net effect of MKP-1 was antiapoptotic, which suggests that the three-drug combination of a proteasome inhibitor, anthracycline, and ERK pathway inhibitor which would further repress MKP-1, may be of interest for patients with breast malignancies. In addition, because MKP-1 is induced by other genotoxic stressors, such as alkylating agents (Liu et al., 1995), it is tempting to speculate that the efficacy of one of the more common regimens used in breast cancer therapy combining doxorubicin and cyclophosphamide is the result of suppression of alkylating agent-mediated induction of antiapoptotic MKP-1. Finally, because MKP-1 is overexpressed even at baseline in a large proportion of primary breast tumor samples (Loda et al., 1996; Wang et al., 2003) and may mediate, in part, glucocorticoid-regulated survival pathways (Wu et al., 2004), it merits further investigation as a mechanism of breast cancer chemoresistance against other drugs that activate JNK, such as taxanes.

Acknowledgments

We acknowledge the generosity of Dr. Tomas Berl (University of Colorado Health Sciences Center, Denver, CO) for the gift of pLNCX and pLNCX- DN-JNK-1α, Dr. Michael J. Birrer (National Cancer Institute, Rockville, MD) for the gift of retroviral supernatants containing pLRT-GFP and pLRT-c-Jun-TAM-67 as well as the pcDNA3.1 and pcDNA3.1-TAM-67 plasmids, Dr. Channing Der (University of North Carolina at Chapel Hill, Chapel Hill, NC) for the gift of pcGN-DP-ERK-1 and -2, and Dr. Philip J. S. Stork (Oregon Health Sciences University, Portland, OR) for the gift of the pcDNA3 and pcDNA3/MKP-1 plasmids. In addition, we greatly thank Dr. Bahadur Singh (University of North Carolina at Chapel Hill) for his statistical theory assistance.

References

Adams J, Palombella VJ, Sausville EA, Johnson J, Destree A, Lazarus DD, Maas J, Pien CS, Prakash S, and Elliott PJ (1999) Proteasome inhibitors: a novel class of potent and effective anti-tumor agents. *Cancer Res* **59:**2615–2622.

Bonni A, Brunet A, West AE, Datta SR, Takasu MA, and Greenberg ME (1999) Cell survival promoted by the Ras-MAPK signaling pathway by transcription-dependent and -independent mechanisms. *Science (Wash DC)* **286:**1358–1362.

Camps M, Nichols A, and Arkinstall S (2000) Dual specificity phosphatases: a gene family for control of MAP kinase function. *FASEB J* **14:**6–16.

Chauhan D, Li G, Hideshima T, Podar K, Mitsiades C, Mitsiades N, Catley L, Tai YT, Hayashi T, Shringarpure R, et al. (2003a) HSP-27 inhibits release of mitochondrial protein Smac in multiple myeloma cells and confers dexamethasone resistance. *Blood* **102:**3379–3386.

Chauhan D, Li G, Shringarpure R, Podar K, Ohtake Y, Hideshima T, and Anderson KC (2003b) Blockade of HSP-27 overcomes bortezomib/proteasome inhibitor PS-341 resistance in lymphoma cells. *Cancer Res* **63:**6174–6177.

Ciechanover A, Orian A, and Schwartz AL (2000) Ubiquitin-mediated proteolysis: biological regulation via destruction. *Bioessays* **22:**442–451.

Franklin CC and Kraft AS (1997) Conditional expression of the mitogen-activated protein kinase (MAPK) phosphatase MKP-1 preferentially inhibits p38 MAPK and stress-activated protein kinase in U937 cells. *J Biol Chem* **272:**16917–16923.

Franklin CC, Srikanth S, and Kraft AS (1998) Conditional expression of mitogen-activated protein kinase phosphatase-1, MKP-1, is cytoprotective against UV-induced apoptosis. *Proc Natl Acad Sci USA* **95:**3014–3019.

Guo YL, Kang B, and Williamson JR (1998) Inhibition of the expression of mitogen-activated protein phosphatase-1 potentiates apoptosis induced by tumor necrosis factor-α in rat mesangial cells. *J Biol Chem* **273:**10362–10366.

Guzman ML, Swiderski CF, Howard DS, Grimes BA, Rossi RM, Szilvassy SJ, and Jordan CT (2002) Preferential induction of apoptosis for primary human leukemic stem cells. *Proc Natl Acad Sci USA* **99:**16220–16225.

Hideshima T, Mitsiades C, Akiyama M, Hayashi T, Chauhan D, Richardson P, Schlossman R, Podar K, Munshi NC, Mitsiades N, et al. (2003) Molecular mechanisms mediating anti-myeloma activity of proteasome inhibitor PS-341. *Blood* **101:**1530–1534.

Kelly K and Chu Y (2000) The regulation of MAP kinase pathways by MAP kinase phosphatases, in *Signaling Networks and Cell Cycle Control* (Gutkind JS ed) pp 165–82, Humana Press, Totowa, NJ.

Li J, Gorospe M, Hutter D, Barnes J, Keyse SM, and Liu Y (2001) Transcriptional induction of MKP-1 in response to stress is associated with histone H3 phosphorylation-acetylation. *Mol Cell Biol* **21:**8213–8224.

Liu Y, Gorospe M, Yang C, and Holbrook NJ (1995) Role of mitogen-activated protein kinase phosphatase during the cellular response to genotoxic stress. Inhibition of c-Jun N-terminal kinase activity and AP-1-dependent gene activation. *J Biol Chem* **270:**8377–8380.

Loda M, Capodieci P, Mishra R, Yao H, Corless C, Grigioni W, Wang Y, Magi-Galluzzi C, and Stork PJ (1996) Expression of mitogen-activated protein kinase phosphatase-1 in the early phases of human epithelial carcinogenesis. *Am J Pathol* **149:**1553–1564.

Ma MH, Yang HH, Parker K, Manyak S, Friedman JM, Altamirano C, Wu ZQ, Borad MJ, Frantzen M, Roussos E, et al. (2003) The proteasome inhibitor PS-341 markedly enhances sensitivity of multiple myeloma tumor cells to chemotherapeutic agents. *Clin Cancer Res* **9:**1136–1144.

Meriin AB, Gabai VL, Yaglom J, Shifrin VI, and Sherman MY (1998) Proteasome inhibitors activate stress kinases and induce HSP-72. Diverse effects on apoptosis. *J Biol Chem* **273:**6373–6379.

Mimnaugh EG, Xu W, Vos M, Yuan X, Isaacs JS, Bisht KS, Gius D, and Neckers L (2004) Simultaneous inhibition of HSP-90 and the proteasome promotes protein ubiquitination, causes endoplasmic reticulum-derived cytosolic vacuolization, and enhances anti-tumor activity. *Mol Cancer Ther* **3:**551–556.

Mitsiades N, Mitsiades CS, Richardson PG, Poulaki V, Tai YT, Chauhan D, Fanourakis G, Gu X, Bailey C, Joseph M, et al. (2003) The proteasome inhibitor PS-341 potentiates sensitivity of multiple myeloma cells to conventional chemotherapeutic agents: therapeutic applications. *Blood* **101:**2377–2380.

Orlowski M and Wilk S (2000) Catalytic activities of the 20 S proteasome, a multicatalytic proteinase complex. *Arch Biochem Biophys* **383:**1–16.

Orlowski RZ and Dees EC (2003) The role of the ubiquitination-proteasome pathway in breast cancer: applying drugs that affect the ubiquitin-proteasome pathway to the therapy of breast cancer. *Breast Cancer Res* **5:**1–7.

Orlowski RZ, Eswara JR, Lafond-Walker A, Grever MR, Orlowski M, and Dang CV (1998) Tumor growth inhibition induced in a murine model of human Burkitt's lymphoma by a proteasome inhibitor. *Cancer Res* **58:**4342–4348.

Orlowski RZ, Small GW, and Shi YY (2002a) Evidence that inhibition of p44/42 mitogen-activated protein kinase signaling is a factor in proteasome inhibitor-mediated apoptosis. *J Biol Chem* **277:**27864–27871.

Orlowski RZ, Stinchcombe TE, Mitchell BS, Shea TC, Baldwin AS, Stahl S, Adams J, Esseltine DL, Elliott PJ, Pien CS, et al. (2002b) Phase I trial of the proteasome inhibitor PS-341 in patients with refractory hematologic malignancies. *J Clin Oncol* **20:**4420–4427.

Pei XY, Dai Y, and Grant S (2003) The proteasome inhibitor bortezomib promotes mitochondrial injury and apoptosis induced by the small molecule Bcl-2 inhibitor HA14–1 in multiple myeloma cells. *Leukemia* **17:**2036–2045.

Richardson PG, Barlogie B, Berenson J, Singhal S, Jagannath S, Irwin D, Rajkumar SV, Srkalovic G, Alsina M, Alexanian R, et al. (2003) A phase 2 study of bortezomib in relapsed, refractory myeloma. *N Engl J Med* **348:**2609–2617.

Riggs CEJ (1997) Anti-tumor antibiotics and related compounds, in *The Chemotherapy Source Book* (Perry MC ed) pp 345–86, Williams & Wilkins, Baltimore.

Robertson JD, Datta K, Biswal SS, and Kehrer JP (1999) Heat-shock protein 70 anti-sense oligomers enhance proteasome inhibitor-induced apoptosis. *Biochem J* **344:**477–485.

Robertson T, Wright FT and Dykstra RL (1988) (eds) *Order Restricted Statistical Inference.* Wiley and Sons, New York, NY.

Scheid MP, Schubert KM, and Duronio V (1999) Regulation of Bad phosphorylation and association with Bcl-x_L by the MAPK/ERK kinase. *J Biol Chem* **274:**31108–31113.

Small GW, Somasundaram S, Moore DT, Shi YY, and Orlowski RZ (2003) Repression of mitogen-activated protein kinase (MAPK) phosphatase-1 by anthracyclines contributes to their anti-apoptotic activation of p44/42-MAPK. *J Pharmacol Exp Ther* **307:**861–869.

Somasundaram S, Edmund NA, Moore DT, Small GW, Shi YY, and Orlowski RZ (2002) Dietary curcumin inhibits chemotherapy-induced apoptosis in models of human breast cancer. *Cancer Res* **62:**3868–3875.

Tournier C, Hess P, Yang DD, Xu J, Turner TK, Nimnual A, Bar-Sagi D, Jones SN, Flavell RA, and Davis RJ (2000) Requirement of JNK for stress-induced activation of the cytochrome c-mediated death pathway. *Science (Wash DC)* **288:**870–874.

Tsuruta F, Sunayama J, Mori Y, Hattori S, Shimizu S, Tsujimoto Y, Yoshioka K, Masuyama N, and Gotoh Y (2004) JNK promotes Bax translocation to mitochondria through phosphorylation of 14-3-3 proteins. *EMBO J* **23:**1889–1899.

Voorhees PM, Dees EC, O'Neil B, and Orlowski RZ (2003) The proteasome as a target for cancer therapy. *Clin Cancer Res* **9:**6316–6325.

Wang HY, Cheng Z, and Malbon CC (2003) Overexpression of mitogen-activated protein kinase phosphatases MKP1, MKP2 in human breast cancer. *Cancer Lett* **191:**229–237.

Wu W, Chaudhuri S, Brickley DR, Pang D, Karrison T, and Conzen SD (2004) Microarray analysis reveals glucocorticoid-regulated survival genes that are associated with inhibition of apoptosis in breast epithelial cells. *Cancer Res* **64:**1757–1764.

Yang Y, Ikezoe T, Saito T, Kobayashi M, Koeffler HP, and Taguchi H (2004) Proteasome inhibitor PS-341 induces growth arrest and apoptosis of non-small cell lung cancer cells via the JNK/c-Jun/AP-1 signaling. *Cancer Sci* **95:**176–180.

Yu C, Rahmani M, Dent P, and Grant S (2004) The hierarchical relationship between MAPK signaling and ROS generation in human leukemia cells undergoing apoptosis in response to the proteasome inhibitor bortezomib. *Exp Cell Res* **295:**555–566.

Address correspondence to: Dr. Robert Z. Orlowski, University of North Carolina at Chapel Hill, 22-003 Lineberger Comprehensive Cancer Center, CB # 7295, Mason Farm Road, Chapel Hill, NC 27599-7295. E-mail: r_orlowski@med.unc.edu